RSC Advances

PAPER

View Article Online
View Journal | View Issue

Cite this: *RSC Adv.*, 2017, **7**, 7734

Selective fluorescent turn-off sensing of Pd^{2+} ion: applications as paper strips, polystyrene films, and in cell imaging†

Pramod Kumar, Vijay Kumar and Rajeev Gupta*

Received 30th November 2016
Accepted 11th January 2017

DOI: 10.1039/c6ra27565f

www.rsc.org/advances

Pyridine-2,6-dicarboxamide based scaffolds with appended naphthyl groups act as fluorescent probes for the selective detection of Pd^{2+} ions in aqueous medium. Collective studies comprising Job's plots, Benesi–Hildebrand fittings, Stern–Volmer plots and detection limits illustrate the notable sensing abilities of such probes for the Pd^{2+} ion. These probes further demonstrate potential applications as paper-strip sensors, as polystyrene film-based sensors, and in cell imaging.

Introduction

The development of sensitive yet selective fluorescent diagnostics for heavy and late transition metal ions is of immense interest due to the profuse use of such metals in various industrial and commercial applications.[1,2] For example, palladium plays an important role in the production of dental and medical devices, jewelry, automobiles and as indispensable catalysts in numerous organic reactions.[3,4] There always exists the possibility of an environmental hazard if the metal is not fully recovered and is released into the surroundings.[5,6] Such a situation poses a significant threat to flora and fauna including humans.[5,6] It is well established that palladium binds to thiol-containing amino acids and protein side chains.[7] As a result, palladium raises significant health concerns due to its ability to perturb various cellular processes even when present in trace concentrations.[7b] It is therefore highly desirable to develop simple yet effective methods to detect residual palladium contamination.[7b,8]

There are several analytical techniques for the detection of Pd^{2+} ion;[9] however, fluorescent-based sensing has received great attention due to its high sensitivity and convenience to operate in biological samples.[10] On the basis of coordination preference of Pd^{2+} ion, chelate-based fluorescent sensors[11–13] as well as chemical reaction based sensors[14,15] have been designed for its detection. Pyridine-2,6-dicarboxamide based scaffolds have been extensively used for coordinating assorted metal ions.[16] We believe that the presence of a chelating cavity endows such scaffolds towards metal binding.[16] However, if such a chelating cavity could also incorporate a suitable fluorophore; then such scaffolds may offer significant sensing possibilities.[17] In this work, we present pyridine-2,6-dicarboxamide based fluorescent probes, L1–L4, offering a chelating cavity while also incorporating naphthyl groups as the fluorophores (Scheme 1). Such fluorescent probes display selective binding towards Pd^{2+} ion in aqueous medium. We also illustrate the applications of such probes in simple cost-effective paper-strip and polystyrene film based sensing as well as in cell imaging.

Results and discussion

Synthesis and characterization of probes

Fluorescent probes, L1–L4, were synthesized by the coupling of either pyridine-2,6-dicarboxylic acid or 4-hydroxy-pyridine-2,6-dicarboxylic acid with either 1-aminonaphthalene or 1-aminomethylene naphthalene. FTIR spectra of probes L1–L4 show N–H stretches between 3300 to 3385 cm^{-1} (Fig. S1–S4†). Interestingly, probe L4 also displayed O–H signal at 3640 cm^{-1}. The proton NMR spectrum of L1 and L3 displayed only one signal for N–H group at 11.42 and 9.92 ppm, respectively. In contrast, probe L2 showed two signals at 11.34 and 11.63 ppm for two different N–H groups whereas L4 exhibited two resonances at 9.84 and 11.49 ppm assigned to O–H and N–H groups, respectively (Fig. S5–S12†). Both FTIR and ^1H NMR spectra of probes

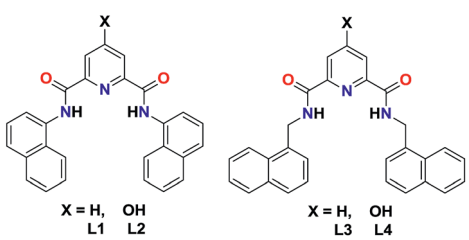

Scheme 1 Chemical drawings of probes L1–L4.

Department of Chemistry, University of Delhi, Delhi 110007, India. E-mail: rgupta@chemistry.du.ac.in; Web: http://people.du.ac.in/~rgupta/; Tel: +91-11-27666646

† Electronic supplementary information (ESI) available: Figures for NMR, FTIR, mass, absorption, and emission spectra, binding constants, detection limit, optical images. CCDC 1455263. For ESI and crystallographic data in CIF or other electronic format see DOI: 10.1039/c6ra27565f

L2 and L4 suggest the occurrence of their tautomeric forms. In the UV-Vis spectrum recorded in DMF, probes L1 and L2 display absorption maxima at *ca.* 295 nm whereas L3 and L4 exhibited λ_{max} at *ca.* 280 nm (Fig. S13a†).

Detection of Pd^{2+} ion

Fluorescent spectral studies on probes L1–L4 in presence of several metal ion were performed in HEPES buffer containing 1% DMF (10 mM, pH = 7.2). Probes L1 and L2 showed emission at 455 and 460 nm respectively after excitation at 310 nm. On the other hand, probes L3 and L4 exhibited prominent emission at 395 and 406 nm respectively after being excited at 290 nm (Fig. S13b†). Although placement of OH group at the *para* position of pyridine ring resulted in red-shift of the emission band but considerably reduced the emission intensity (Fig. S13b†). Under the identical conditions, fluorescence quantum yields of probes L1–L4 were measured using 2-aminopyridine as a reference ($\Phi_S = 0.6$).[18] The quantum yields of probes L1–L4 were found to be 0.0044, 0.0026, 0.0083 and 0.0068, respectively. A comparison suggests that the introduction of OH group at the *para* position of pyridine ring has reduced the fluorescence quantum yield of probes L2 and L4 when compared to L1 and L3, respectively.

Addition of five equivalents of various metal ion, such as Na^+, Ca^{2+}, Cr^{3+}, Fe^{2+}, Fe^{3+}, Mn^{2+}, Co^{2+}, Ni^{2+}, Cu^{2+}, Zn^{2+}, Ag^+, Cd^{2+}, Hg^{2+}, Pb^{2+}, Pt^{2+}, Au^{3+}, and Al^{3+} did not significantly perturb the emission intensity of probes L1–L4. However, presence of Pd^{2+} ion quenches the emission intensity to great extent (Fig. 1 and S14 and S15†). A comparison of four probes, L1–L4, illustrates that L3 and L4 not only exhibited remarkable emission but also much larger quenching as compared to probes L1 and L2 (Fig. S16†). Hence, probes L3 and L4 were selected for the further studies.

The change in fluorescence intensity of probes L3 and L4 were investigated by the incremental addition of Pd^{2+} ion which resulted in quantitative quenching (Fig. 2a and b). The quenching efficiency can be conveniently interpreted by calculating the Stern–Volmer constants (K_{SV}).[19] The Stern–Volmer plots provided K_{SV} values of 4.48×10^4 and 2.89×10^4 M^{-1} for probes L3 and L4, respectively (Fig. 2c). Further, both fluorescent probes L3 and L4 showed noteworthy detection limits of 0.78 and 0.93 μM respectively for Pd^{2+} ion (Fig. S17†). Both K_{SV} values as well as detection limits indicate that the probe L3 caused maximum quenching as compared to probe L4. Notably, Pd^{2+} detection limits of probes L3 and L4 are much better than its threshold limit of 47.0–94.0 μM in drugs and chemicals recommended by WHO.[7b,11a] Importantly, advanced analytical methods, such as atomic absorption spectrometry, inductively coupled plasma optical emission spectrometry, inductively coupled plasma mass spectrometry, and X-ray fluorescence spectroscopy, used for the quantification of palladium require sophisticated instrumentation, complicated sample preparation, rigorous experimental conditions, and well-trained individuals while the present method relies on a simple fluorescence technique.[9] Time-resolved fluorescence studies explained the excited state behavior of probe L3 in the absence

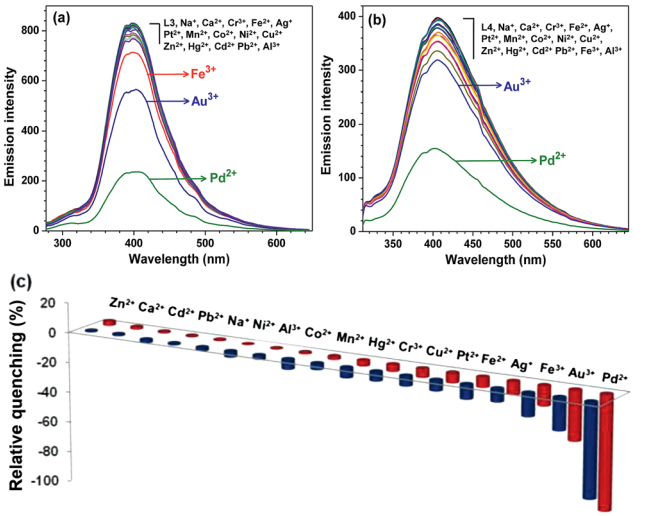

Fig. 1 Emission spectra of probe (a) L3 and (b) L4 (50 μM) in HEPES buffer containing 1% DMF (10 mM, pH = 7.2) and after their interaction with assorted metal ions (250 μM). (c) Bar diagram exhibiting relative quenching at 395 nm for probe L3 (red pillars) and at 406 nm for probe L4 (blue pillars) after the addition of assorted metal ions (250 μM).

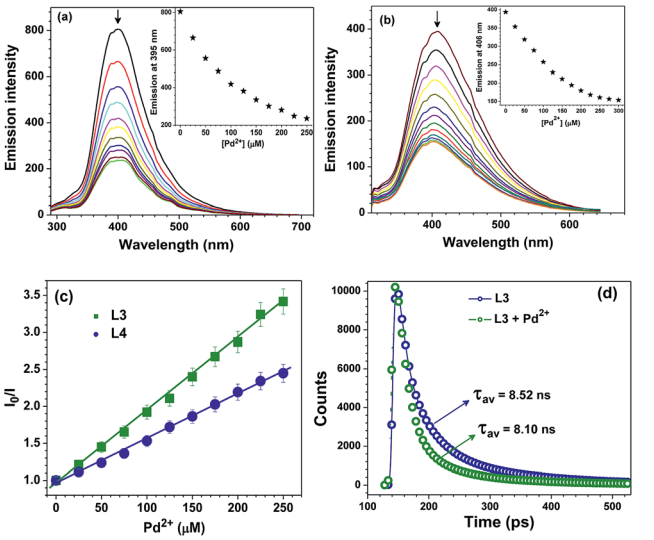

Fig. 2 Change in emission intensity with the number of equivalents (0–5 equivalents) of Pd^{2+} ion for probes (a) L3 (50 μM) and (b) L4 (50 μM) in HEPES buffer containing 1% DMF (10 mM, pH = 7.2). Insets: change in emission intensity at 395 nm for L3 (a) and 406 nm for L4 (b) with the number of equivalents (0–5 equivalents) of Pd^{2+} ion. (c) Stern–Volmer plots for probes L3 (green squares) and L4 (blue spheres) with Pd^{2+} ion. (d) Lifetime profile of probe L3 in absence and presence Pd^{2+} ion in HEPES buffer (10 mM, pH = 7.2) (λ_{ex} = 280 nm λ_{em} = 395 nm).

and presence of Pd^{2+} ion in buffer solution (Fig. 2d).[20] The decay profile of probe L3 exhibited a tri-exponential decay with average lifetime of τ_{av} = 8.52 ns. With the addition of 5 equivalents of Pd^{2+} ion, the average lifetime of probe L3 showed a decrease (τ_{av} = 8.10 ns). Such a fact suggests complexation of Pd(II) ion with probe L3 which agrees well with other studies (*vide infra*).

Selectivity studies for Pd^{2+} ion

It is desirable for a good chemosensor to show fast response and high sensitivity in addition to high degree of selectivity. To evaluate the interference from other metal ions in the detection of Pd^{2+} ion, competitive binding studies were investigated in presence of following metal ions: Na^{+}, Ca^{2+}, Cr^{3+}, Fe^{2+}, Fe^{3+}, Mn^{2+}, Co^{2+}, Ni^{2+}, Cu^{2+}, Zn^{2+}, Ag^{+}, Cd^{2+}, Hg^{2+}, Pb^{2+}, Pt^{2+}, Au^{3+}, and Al^{3+}. For such competitive binding studies, matching concentrations of Pd^{2+} ion and other metal ions were tested. Fig. 3 nicely illustrates that no other metal ion effectively intervened with the Pd^{2+} ion detection suggesting that both probes L3 and L4 function as the selective sensors for the detection of Pd^{2+} ion even in presence of other potential metal ions. We also investigated the change in emission intensity of probes L3 and L4 in presence of different palladium salts such as $PdCl_2$, $Pd(CH_3COO)_2$, $Pd(NO_3)_2$ and K_2PdCl_4 (Fig. S18†). Notably, all four palladium salts showed a very similar quenching in the emission intensity of probes L3 and L4, thus suggesting no prominent role of the associated anion.

Binding stoichiometry for Pd^{2+} ion

The binding stoichiometry and association constants for naphthyl-methylene based probes L3 and L4 were investigated from Job's plots[21] as well as Benesi–Hildebrand plots[22] using fluorescence measurement. Using Job's method of continuous variation of mole fraction, a stoichiometry of 1 : 1 was observed for Pd^{2+} ion with probes L3 and L4 (Fig. S19†).[17] The binding stoichiometry was further investigated by the Benesi–Hildebrand fitting which additionally supported a 1 : 1 stoichiometry.[17] The binding constants, K_b, computed for Pd^{2+} ion were $7.68 \times 10^3\ M^{-1}$ and $2.92 \times 10^3\ M^{-1}$ for L3 and L4 respectively using the Benesi–Hildebrand method (Fig. S20†). Both Job's plot and Benesi–Hildebrand method inferred a 1 : 1 stoichiometry and formation of [Pd–L3] and [Pd–L4] complexes of Pd^{2+} ion with probes L3 and L4, respectively. The formation of [Pd–L3] and [Pd–L4] was further investigated by the UV-Vis spectral titrations. The change in absorption spectra by the addition of Pd^{2+} ion suggested the interaction of Pd^{2+} ion with probes L3 and L4 (Fig. S21†). These studies further supported the emission spectral titrations.

Isolation of complex 1

To gain a conclusive insight, we attempted to isolate the product from the reaction between Pd^{2+} ion and L3 as this probe provided the best detection results. A white product was isolated when probe L3 was treated with $Pd(CH_3COO)_2$ in DMF/H_2O. Subsequent recrystallization from MeCN afforded a crystalline product, namely complex **1**. FTIR spectrum of **1** showed the disappearance of N–H peaks and red-shifted O_{amide} bands; both inferring coordination of Pd(II) ion by the deprotonated form of probe L3 (Fig. S22†).[23] Further, C≡N stretches for the coordinated CH_3CN were clearly visible between 2325–2298 cm^{-1}. ^1H NMR spectrum of **1** further confirmed the disappearance of N–H signals whereas coordinated CH_3CN was noted at 2.04 ppm (Fig. S23†). Complex **1** was crystallographically characterized and the molecular structure is shown in Fig. 4. The Pd(II) ion adopts a distorted square-planar geometry coordinated within the N_3 pincer cavity created by a $N_{pyridine}$ and two N_{amide} atoms.[24] The fourth coordination is provided by an acetonitrile molecule. As anticipated, complex **1** is fluorescence inactive in solution (Fig. S24†) as well as in the solid state.

Fabrication of filter paper strips and polystyrene films

Despite notable work on sensing of palladium, straight-forward and cost-effective detection methods still remain a challenge.[12f,25] Such an approach will be beneficial for an effective

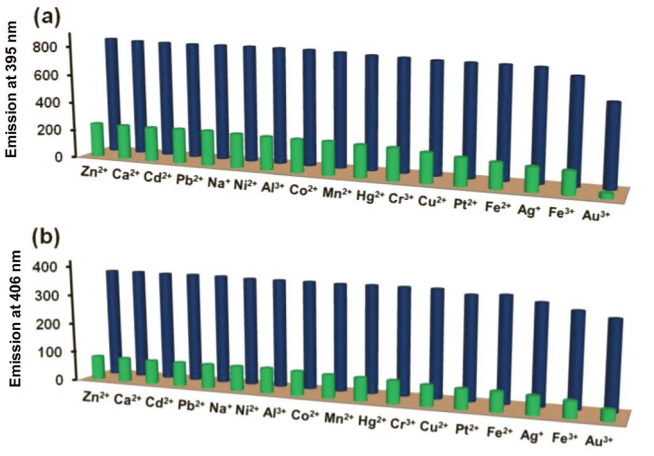

Fig. 3 Selectivity of Pd^{2+} ion *versus* other metal ions: (a) L3 + other metal ions (blue pillars) and L3 + other metal ions + Pd^{2+} ion (green pillars); (b) L4 + other metal ions (blue pillars) and L4 + other metal ions + Pd^{2+} ion (green pillars).

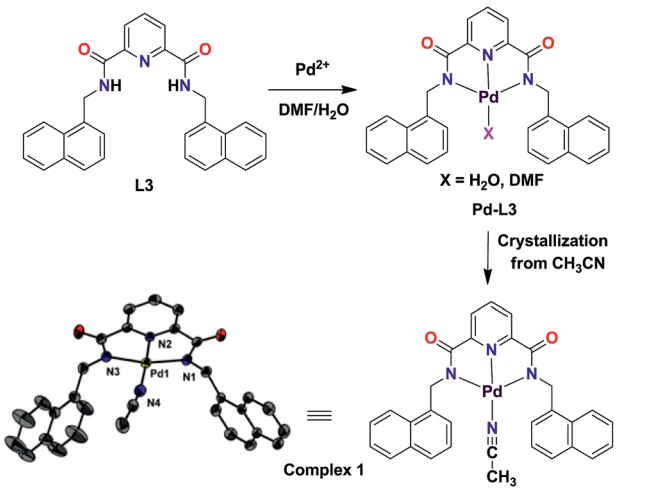

Fig. 4 Proposed reaction of probe L3 with Pd^{2+} ion in H_2O/DMF and the isolated and structurally characterized complex **1** (30% thermal ellipsoidal representation whereas hydrogen atoms have been omitted for clarity). Selected bond distances (Å): Pd–N1 = 2.017(3), Pd–N2 = 1.917(3), Pd–N3 = 2.020(3), Pd–N4 = 2.014(4). Selected bond angles (°): N1–Pd1–N2 = 80.71(13), N2–Pd1–N3 = 81.12(13), N1–Pd1–N3 = 161.79(13), N2–Pd1–N4 = 177.14(13), N1–Pd1–N4 = 101.91(14), N3–Pd1–N4 = 96.29(14).

detection under various experimental conditions. In this context, we attempted to fabricate filter paper test strips containing probes L3 and L4 due to their promising emission properties. The filter paper strips were coated with probes by immersing them in HEPES buffer solutions of L3 and L4 (containing 1% DMF, 10 mM, pH = 7.2) followed by drying in air. Such test strips were used directly by dipping them into an aqueous solution of any Pd(II) salt. As can be seen from Fig. 5, both probes were quite effective in detecting Pd^{2+} ion from the aqueous solutions.

We also fabricated peelable polystyrene films by doping probes L3 and L4 during their synthesis.[17a] Such films were used for the detection of Pd^{2+} ion from the aqueous medium as illustrated in Fig. 6. Notably, these polystyrene films provided options to fabricate cheap yet mouldable options for sensing Pd^{2+} ion from the aqueous medium.

Cytotoxicity and cell imaging

The Pd^{2+} ion is toxic to living organism; therefore, its detection inside a cell would be an important factor to ascertain the efficiency of probes L3 and L4. However, before going to cell imaging, cytotoxicity activities of probes L3 and L4 in presence/absence of Pd^{2+} ion for HEK-293 and L929 cell lines were investigated using MTT assay.[26] *In vitro* cytotoxicity against HEK-293 and L929 cells in terms of IC_{50} values is presented in Fig. 7 and compared with the anti-cancer drug cis-platin. The

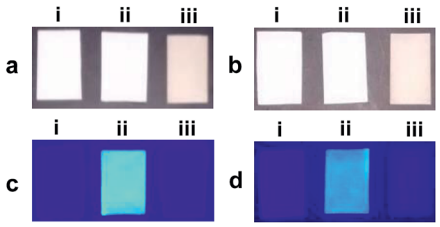

Fig. 5 (a) Images of filter paper strips: (a, b) and (c, d) are the images of filter paper strips in visible and ultraviolet region, respectively. In all cases, (i) exhibits images for only filter paper strips, (ii) exhibits images after treatment with probe L3 (a and c) and L4 (b and d), whereas (iii) display images of test strips coated with L3 (a and c) and L4 (b and d) and after treatment with aqueous Pd^{2+} ion.

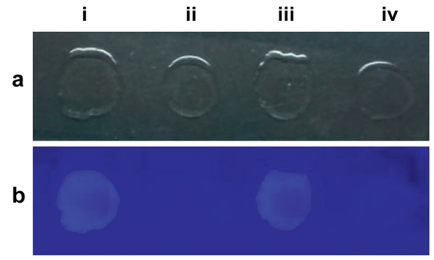

Fig. 6 (a) Images of polystyrene films on a glass slide in (a) visible and (b) ultraviolet region. In all cases, (i) and (iii) exhibit the images of films containing probe L3 and L4, respectively; whereas (ii) and (iv) exhibit the images of same films after treating with an aqueous solution of Pd^{2+} ion.

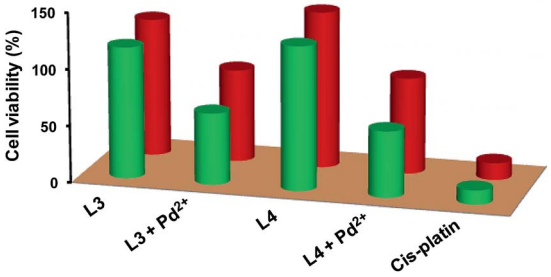

Fig. 7 Bar diagram showing IC_{50} values of *in vitro* cytotoxicity assay for HEK-293 (red pillars) and L929 cells (green pillars). IC_{50} values for HEK-293 cells: 122.4 (L3); 82.1 (L3 + Pd^{2+}); 138.7 (L4); 85.1 (L4 + Pd^{2+}); 14.9 (cis-platin). IC_{50} values for L929 cells: 116.3 (L3); 63.3 (L3 + Pd^{2+}); 127.4 (L4); 58.5 (L4 + Pd^{2+}); 12.5 (cis-platin).

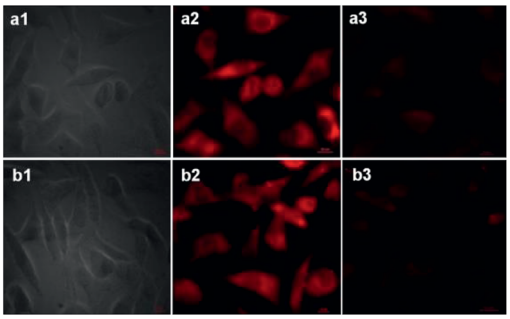

Fig. 8 Fluorescence microscopic images (100×) of L929 cells after 90 minutes incubation: (a1) and (b1) bright field images of cells treated with probes L3 and L4 (50 μM), respectively; (a2) and (b2) red channel images of cells treated with L3 and L4 (50 μm), respectively; (a3) and (b3) cells treated with L3 and L4 (50 μM), respectively and with Pd^{2+} ion (250 μM).

results exhibit that probes L3 and L4 are very less cytotoxic in absence of Pd^{2+} ion. Although, presence of Pd^{2+} ion somewhat increases the cytotoxicity against both cell lines; the probe-Pd combinations are still quite safe than that of cis-platin. These experiments also suggest that both probes L3 and L4 are able to penetrate the cell wall without causing any damage to the cells.

The cell-imaging experiments were performed to ascertain whether probes L3 and L4 are able to detect Pd^{2+} ion in living cells. Thus, when L929 cells were incubated with probes L3 or L4 (50 μM) at 37 °C for 90 min, these cells showed an intense fluorescence (Fig. 8, panels a2 and b2). After being treated with Pd^{2+} ion (250 μM) for 90 min at 37 °C; these cells showed negligible fluorescence (Fig. 8, panels a3 and b3). These experiments assert that both probes L3 and L4 are able to detect Pd^{2+} ion in the biological samples.

Conclusions

In conclusion, a series of pincer cavity based probes (L1–L4) has been developed for the selective detection of Pd^{2+} ion. Fluorescence quenching, Stern–Volmer plots and detection limits advocated strong sensing abilities of probes L3 and L4 for Pd^{2+} ion. The Pd^{2+} ion was found to bind with probes L3 and L4 by

forming a 1 : 1 complex, a fact proved by the crystal structure of [L3–Pd] complex. Filter paper test strips and polystyrene based films validated the cost-effective detection methods for Pd^{2+} ion. Probes L3 and L4 were also utilized for the fluorescence based cell imaging and the results were supplemented with cell viability studies. This report illustrates a simple strategy of developing pincer-cavity based selective probes for palladium ion and may find application in tracking palladium as well as other toxic metals ions in industrial affluent and living organism.

Experimental section

Materials

The analytical grade chemicals and metal salts were used as received without further purifications. High quality HPLC grade solvents were used for the UV-Vis and fluorescence spectral measurements. The probes L1 and L3 are reported in literature but have been synthesized using different synthetic methods.[27] However, in the present manuscript; all four probes L1–L4 have been synthesized in high yield using a common procedure. HEK-293 (human embryonic kidney cells 293) and L929 cells (murine cells) were obtained from the National Center for Cell Science (NCCS), Pune, India. MTT (3-(4,5-dimethyl-2-thiazolyl)-2,5-diphenyltetrazolium bromide) and cell culture grade DMSO were obtained from the Himedia (Mumbai, India). Injectable cisplatin was obtained from the Ranbaxy (Mumbai, India).

Physical measurements

Elemental analysis data were obtained from the Elementar Analysen Systeme GmbH Vario EL-III instrument. The ^{1}H and ^{13}C NMR spectra were recorded with a JEOL 400 MHz NMR instrument. FTIR spectra were recorded using a Perkin-Elmer Spectrum-Two spectrometer having Zn–Se ATR. The absorption spectra were measured with a Perkin-Elmer Lambda-25 spectrophotometer. Fluorescence spectral studies were performed with a Cary Eclipse fluorescence spectrophotometer. ESI-MS mass spectra were obtained with Agilent Q-TOF LC-MS mass spectrometer. Time-resolved fluorescence spectra were recorded using a picosecond fluorimeter from Horiba Jobin Yvon (FluoroHub).

Synthesis of probes and complexes

Probe L1. A mixture of pyridine-2,6-dicarboxylic acid (1.0 g, 0.0059 mol) and 1-aminonaphthalene (1.689 g, 0.0118 mol) was taken in 25 mL pyridine and refluxed for 30 min at 120 °C. $P(OPh)_3$ (3.877 g, 0.0125 mol) was added drop-wise and the reaction mixture was finally stirred at 80 °C for 12 h. After cooling to room temperature, the mixture was poured into an ice-cold water that caused precipitation of an off-white product. The product was filtered, washed with water followed by ethanol several times and dried under vacuum. Yield: 2.16 g (88%). Anal. calc. for $C_{27}H_{19}N_3O_2$: C, 77.68; H, 4.59; N, 10.07. Found: C, 77.65; H, 4.54; N, 10.02. FTIR spectrum (Zn–Se ATR, cm^{-1}): 3302 (N–H), 1664, 1543. UV/Vis spectrum (DMF, ε, M^{-1} cm^{-1}): λ_{max} 294 (14 760). ^{1}H NMR spectrum (400 MHz, DMSO-d_6): $\delta = 11.42$ (s, 1H), 8.42 (d, $J = 7.60$ Hz, 2H), 8.72 (t, $J = 7.20$ Hz, 1H), 8.08 (d, $J = 8.0$ Hz, 2H), 7.97 (d, $J = 8.0$ Hz, 2H), 7.88 (d, $J = 8.0$ Hz, 2H), 7.67 (d, $J = 6.80$ Hz, 2H), 7.60–7.52 (m, 6H). ^{13}C NMR spectrum (100 MHz, DMSO-d_6): 163.19, 149.30, 140.65, 134.28, 133.57, 129.89, 128.69, 127.27, 126.83, 126.16, 125.85, 124.90, 123.87, 115.74.

Probe L2. Probe L2 was synthesized in a similar manner as discussed for probe L1, however, with following reagents: 4-hydroxy-pyridine-2,6-dicarboxylic acid (1.0 g, 0.0054 mol), 1-aminonaphthalene (1.544 g, 0.0108 mol), and $P(OPh)_3$ (3.877 g, 0.0125 mol). Yield: 1.98 g (85%). Anal. calc. for $C_{27}H_{19}N_3O_3$: C, 74.81; H, 4.42; N, 9.69. Found: C, 74.85; H, 4.48; N, 9.72. FTIR spectrum (Zn–Se ATR, cm^{-1}): 3322 (N–H), 1672, 1656, 1535. UV/Vis spectrum (DMF, ε, M^{-1} cm^{-1}): λ_{max} 295 (14 940). Mass spectrum (ESI^+, MeOH, m/z): calc. 433.1426 for L2; found 434.1502 for L2 + H^+. ^{1}H NMR spectrum (400 MHz, DMSO-d_6): $\delta = 11.63$ (s, 1H), 11.34 (s, 2H), 8.06 (d, $J = 8.01$ Hz, 2H), 7.96 (d, $J = 7.60$ Hz, 2H), 7.87 (d, $J = 8.03$ Hz, 2H), 7.75 (s, 2H), 7.66 (d, $J = 6.81$ Hz, 2H), 7.60–7.52 (m, 6H). ^{13}C NMR spectrum (100 MHz, DMSO-d_6): 167.5, 163.2, 151.3, 134.2, 133.6, 129.8, 128.6, 127.1, 126.8, 126.7, 126.1, 124.7, 123.8, 112.8.

Probe L3. Probe L3 was synthesized in a similar manner as discussed for probe L1, however, using the following reagents: pyridine-2,6-dicarboxylic acid (1.0 g, 0.0059 mol), 1-amino-methylenenaphthalene (1.85 g, 0.0118 mol), and $P(OPh)_3$ (3.877 g, 0.0125 mol). Yield: 2.35 g (90%). Anal. calc. for $C_{29}H_{23}N_3O_2$: C, 78.18; H, 5.20; N, 9.53. Found: C, 78.13; H, 5.16; N, 9.48. FTIR spectrum (Zn–Se ATR, cm^{-1}): 3285 (N–H), 1653, 1520. UV/Vis spectrum (DMF, ε, M^{-1} cm^{-1}): λ_{max} 280 (18 150). Mass spectrum (ESI^+, MeOH, m/z): calc. 445.1790 for L3; found 446.1866 for L3 + H^+. ^{1}H NMR spectrum (400 MHz, DMSO-d_6): $\delta = 9.92$ (t, $J = 5.60$ Hz, 2H), 8.26 (d, $J = 8.02$ Hz, 2H), 8.20–8.15 (m, 3H), 7.91 (t, $J = 5.22$ Hz, 2H), 7.80 (d, $J = 4.40$ Hz, 2H), 7.50 (t, $J = 4.42$ Hz, 4H), 7.42 (d, $J = 6.42$ Hz, 4H), 5.03 (d, $J = 6.02$ Hz, 4H). ^{13}C NMR spectrum (100 MHz, DMSO-d_6): 163.90, 149.20, 140.22, 134.77, 133.77, 131.12, 129.12, 128.00, 126.85, 126.39, 125.97, 125.22, 124.90, 123.75, 115.74, 40.77.

Probe L4. Probe L4 was synthesized in a similar manner as discussed for probe L1, however, using the following reagents: 4-hydroxy-pyridine-2,6-dicarboxylic acid (1.0 g, 0.0054 mol); 1-aminomethylene naphthalene (1.695 g, 0.0108 mol); and $P(OPh)_3$ (3.877 g, 0.0125 mol). Yield: 2.04 g (82%). Anal. calc. for $C_{29}H_{23}N_3O_3$: C, 75.47; H, 5.02; N, 9.10. Found: C, 75.54; H, 5.41; N, 8.82. FTIR spectrum (Zn–Se ATR, cm^{-1}): 3640 (O–H), 3340 (N–H), 1658 (C=O), 1528, 1336. UV/Vis spectrum (DMF, ε, M^{-1} cm^{-1}): λ_{max} 280 (18 350). Mass spectrum (ESI^+, MeOH, m/z): calc. 461.1739 for L4; found 462.1828 for L4 + H^+. ^{1}H NMR spectrum (400 MHz, DMSO-d_6): $\delta = 11.49$ (s, 1H), $\delta = 9.84$ (t, $J = 6.02$ Hz, 2H), 8.16 (d, $J = 6.82$ Hz, 2H), 7.90 (d, $J = 8.81$ Hz, 2H), 7.80 (d, $J = 7.63$ Hz, 2H), 7.61 (s, 2H), 7.50 (t, $J = 4.48$ Hz, 4H), 7.44–7.39 (m, 4H), 5.00 (d, $J = 5.60$ Hz, 4H). ^{13}C NMR spectrum (100 MHz, DMSO-d_6): 167.25, 163.98, 151.22, 134.84, 133.77, 131.13, 129.11, 127.97, 126.84, 126.38, 125.97, 124.91, 123.75, 112.26, 40.76.

Complex 1. Probe L3 (0.10 g, 0.224 mmol) was dissolved in a mixture of H_2O/DMF (1 : 1 v/v, 5 mL) and a solution of

$Pd(CH_3COO)_2$ (0.050 g, 0.224 mmol) in 2 mL H_2O was added drop-wise. The reaction mixture was stirred for 2 h under ambient conditions. The solvent was evaporated under the reduced pressure to obtain a pale yellow solid. Yellow crystalline product was obtained within a day by the slow evaporation of an acetonitrile solution of the crude product. Yield: 0.108 g (82%). Anal. calc. for $C_{31}H_{24}N_4O_2Pd$: C, 63.00; H, 4.09; N, 9.48. Found: C, 63.06; H, 4.12; N, 9.53. FTIR spectrum (Zn–Se ATR, cm^{-1}): 2325, 2298 ($C{\equiv}N_{CH_3CN}$), 1601 (C=O), 1374. ^1H NMR spectrum (400 MHz, DMSO-d_6): $\delta = 8.23$ (t, $J = 6.88$ Hz, 1H), 8.09 (d, $J = 6.87$ Hz, 2H), 7.90 (d, $J = 7.64$ Hz, 2H), 7.77–7.71 (m, 6H), 7.55–7.45 (m, 6H), 4.74 (s, 4H), 2.04 (s, 3H).

General methods and determination of constants

All stock solutions (10 mM) of metal ions Na^+, Ca^{2+}, Cr^{3+}, Fe^{2+}, Fe^{3+}, Mn^{2+}, Co^{2+}, Ni^{2+}, Cu^{2+}, Zn^{2+}, Ag^+, Cd^{2+}, Hg^{2+}, Pb^{2+}, Pd^{2+}, Pt^{2+}, Au^{3+}, and Al^{3+} were prepared in H_2O or DMF according to their solubility. All UV-Vis and fluorescence spectra were recorded with a cuvette of 1.0 cm path length at room temperature (25 ± 1 °C).

The fluorescence quantum yields (Φ) for fluorescent probes L1–L4 were calculated using the eqn (1) using 2-aminopyridine as a standard ($\Phi_S = 0.6$) in 0.1 N H_2SO_4.[18]

$$\Phi_X = \Phi_S(I_X/I_S)(A_X/A_S)(\eta_X{}^2/\eta_S{}^2) \quad (1)$$

where, X used for probes L1–L4 and S for standard solution (2-aminopyridine), respectively; Φ = quantum yield; I = area under the fluorescence emission curve; A = absorbance at excitation wavelength; η = refraction index of the solvent.

The Stern–Volmer constants (K_{SV}) were evaluated by a plot between I_0/I and $[Pd^{2+}]$ using Stern–Volmer eqn (2).[19]

$$I_0/I = 1 + K_{SV}[Pd^{2+}] \quad (2)$$

where I_0 and I are fluorescence intensity of probes (L3 and L4) in absence and in the presence of Pd^{2+} ion, respectively.

The detection limit for the detection of Pd^{2+} ion was calculated using the eqn (3).[28]

$$\text{Detection limit: } 3\sigma/k \quad (3)$$

where σ is standard deviation and determined by ten blank replicate measurements of probes L3 or L4 and k is the slope of a plot of fluorescence intensity of L3 or L4 *versus* $[Pd^{2+}]$.

The binding stoichiometry of Pd^{2+} ion with probes L3 and L4 was determined by the Job's plot using mole fraction.[21] The binding constant (K_b) was determined by the Benesi–Hildebrand eqn (4) by plotting $1/(I - I_0)$ against $1/[Pd^{2+}]$.[22]

$$1/(I - I_0) = 1/\{K_b(I_0 - I_{min})[Pd^{2+}]\} + 1/(I_0 - I_{min}) \quad (4)$$

where I is the emission intensity of L3 or L4 in presence of Pd^{2+} ion at 395 nm and 406 nm, respectively; I_0 is the intensity of L3 or L4 in absence of Pd^{2+} ion; and I_{min} is the minimum fluorescence intensity in presence of Pd^{2+} ion. K_b value was obtained by the ratio of intercept and slope of plot $1/(I - I_0)$ *vs.* $1/[Pd^{2+}]$.

Fabrication of filter paper strips

Strips of Whatman filter paper were dipped in a solution of probes L3 or L4 in HEPES buffer solution containing 1% DMF (10 mM, pH = 7.2) and were air-dried to prepare the test strips. Test strips coated with either L3 or L4 were dipped for a few seconds directly into the aqueous solution of palladium acetate. Such paper strips were then investigated under the visible and ultraviolet light.

Fabrication of polystyrene films

A mixture of styrene (0.5 mL) containing α,α′-azoisobutyronitrile (AIBN; 1 mg) and probes L3 or L4 in methanol (0.5 mL) was heated on water bath at 80 °C for 30 min. Subsequently, a few drops of hot clear solution were poured over a glass slide and the resultant glass slide was air dried to produce a film of polystyrene. Such films were peeled off from the glass slide and were used for detecting Pd(II) ion by directing dipping in an aqueous solution of $Pd(CH_3COO)_2$. These polystyrene films were then photographed under the visible and ultraviolet light.

In vitro cytotoxicity assay

The cytotoxicity potentials of probes L3 and L4, in absence and presence of Pd^{2+} ion, were evaluated by the MTT (3-(4,5-dimethylthiazol-2-yl)-2,5-diphenyltetrazolium bromide) assay using L929 and HEK-293 cell line.[26] These cells (1×10^4) were seeded on 96-well plates in growth medium and incubated for 24 h at 37 °C in CO_2 incubator. Serial concentrations of probes L3 and L4 and Pd(II) salt ranging from 0.05–200 μM in DMSO were added to the wells and such well were incubated for next 24 h.[29] MTT labelling mixture (5 mg mL^{-1}) was added to the cells after discarding the medium, and incubated for 2 h at 37 °C. MTT and media were removed and 100 μL of pure DMSO was added to each well plate to dissolve the formazon crystals. The result of MTT assay was expressed in percentage of inhibition and values were determined on Fluostar optima (BMG Labtech, Germany) microplate reader at 570 nm. All experiments were independently repeated three times.

Fluorescence cell imaging

In vitro cell imaging with probes L3 and L4, in absence and presence of Pd^{2+} ion, were analyzed with murine cells L929. The L929 cells were cultured in DMEM growth medium (supplemented with 1% streptomycin as antibiotic) and incubated at 37 °C in CO_2 incubator. Cells were seeded (1.0×10^5 cells per well) in six well plate and incubated at 37 °C for 12 h. Probe L3 and L4 (50 μM) were added to these cells in phosphate buffer saline (PBS) and incubated for 90 min.[30] In an additional set of experiments, cells were incubated with the same probes L3 and L4 (50 μM) however in presence of Pd^{2+} ion (1 mM). After 90 min incubation, cells were washed with PBS to remove the traces of probe L3 and L4. As a final point, the cells were fixed with 4% paraformaldehyde solution and images were acquired using the Upright Microscope (Axio Imager 2.2, Carl Zeiss, Germany).

Table 1 Crystallographic data collection and structure solution parameters for complex 1

Empirical formula	$C_{31}H_{24}N_4O_2Pd$
Formula weight	590.94
T (K)	293(2)
System	Monoclinic
Space group	$P2_1/c$
a (Å)	16.3379(4)
b (Å)	10.9218(3)
c (Å)	15.1158(4)
α (°)	90.00
β (°)	106.795(3)
γ (°)	90.00
V (Å^3)	2582.20(12)
Z	4
ρ_{calc} (mg m^{-3})	1.520
F (000)	1200
Goodness-of-fit (GOF) on F^2	0.980
Final R indices [$I > 2\sigma(I)$]	$R_1 = 0.0442$, w$R_2 = 0.0818$
R indices (all data)[a]	$R_1 = 0.0692$, w$R_2 = 0.0909$
CCDC no.	1455263

[a] $R_1 = \sum||F_o| - |F_c||/\sum|F_o|$; w$R_2 = \{\sum[w(|F_o|^2 - |F_c|^2)^2]/\sum[wF_o^4]\}^{1/2}$.

X-ray crystallography

Single crystals suitable for the X-ray diffraction studies were grown by the slow evaporation of an acetonitrile solution of [Pd–L3] complex. The intensity data were collected at 298 K with an Oxford XCalibur CCD diffractometer equipped with a graphite monochromated Mo-Kα radiation (λ = 0.71073 Å).[31] Data reduction was performed with the CrysAllisPro program (Oxford Diffraction ver. 171.34.40).[31] The structure was solved using the direct methods using SHELXS-97 (ref. 32) and refined on F^2 using all data by full matrix least-squares procedures with SHELXL-97 within the OLEX-2 suite.[33] The hydrogen atoms were placed at the calculated positions and included in the last cycles of the refinement. All calculations were done using the WinGX software package.[34] Crystallographic data collection and structure solution parameters are summarized in Table 1. CCDC-1455263 contains the supplementary crystallographic data for this paper.†

Acknowledgements

PK thanks UGC, New Delhi for the award of Dr D. S. Kothari Postdoctoral fellowship. RG acknowledges the Council of Scientific and Industrial Research (CSIR), New Delhi and the University of Delhi for the financial support. Authors thank the CIF-USIC at this university for the instrumental facilities including crystallographic data collection.

Notes and references

1 (*a*) K. P. Carter, A. M. Young and A. E. Palmer, *Chem. Rev.*, 2014, **114**, 4564; (*b*) J. Chan, S. C. Dodani and C. J. Chang, *Nature*, 2012, **4**, 973; (*c*) X. L. Zhang, Y. Xiao and X. H. Qian, *Angew. Chem., Int. Ed.*, 2008, **47**, 8025.

2 (*a*) E. W. Miller, Q. He and C. J. Chang, *Nat. Protoc.*, 2008, **3**, 777; (*b*) X. Peng, J. Du, J. Fan, J. Wang, Y. Wu, J. Zhao, S. Sun and T. Xu, *J. Am. Chem. Soc.*, 2007, **129**, 1500.

3 (*a*) T. Iwasawa, M. Tokunaga, Y. Obora and Y. Tsuji, *J. Am. Chem. Soc.*, 2004, **126**, 6554; (*b*) M. Lafrance and K. Fagnou, *J. Am. Chem. Soc.*, 2006, **128**, 16496; (*c*) H. Li, J. Fan and X. Peng, *Chem. Soc. Rev.*, 2013, **42**, 7943; (*d*) L. D. Prockop and R. I. Chichkova, *J. Neurol. Sci.*, 2007, **262**, 122.

4 (*a*) X.-F. Wu, H. Neumann and M. Beller, *Chem. Soc. Rev.*, 2011, **40**, 4986; (*b*) R. Jana, T. P. Pathak and M. S. Sigman, *Chem. Rev.*, 2011, **111**, 1417; (*c*) E. M. Beccalli, G. Broggini, M. Martinelli and S. Sottocornola, *Chem. Rev.*, 2007, **107**, 5318.

5 (*a*) T. Z. Liu, S. D. Lee and R. S. Bhatnagar, *Toxicol. Lett.*, 1979, **4**, 469; (*b*) J. C. Wataha and C. T. Hanks, *J. Oral Rehabil.*, 1996, **23**, 309.

6 C. E. Garrett and K. Prasad, *Adv. Synth. Catal.*, 2004, **346**, 889.

7 (*a*) J. Kielhorn, C. Melber, D. Keller and I. Mangelsdorf, *Int. J. Hyg. Environ. Health*, 2002, **205**, 417; (*b*) International Programme on Chemical Safety, *Palladium; Environmental Health Criteria Series 226*, World Health Organization, Geneva, 2002.

8 (*a*) T. Z. Liu, T. F. Lin, D. T. Y. Chiu, K.-J. Tsai and A. Stern, *Free Radical Biol. Med.*, 1997, **23**, 155; (*b*) M. D. Shultz, J. P. Lassid, M. G. Gooch, B. R. Evans and J. Woodward, *Biochem. Biophys. Res. Commun.*, 1995, **209**, 1046.

9 (*a*) K. van Meel, A. Smekens, M. Behets, P. Kazandjian and R. van Grieken, *Anal. Chem.*, 2007, **79**, 6383; (*b*) C. Locatelli, D. Melucci and G. Torsi, *Anal. Bioanal. Chem.*, 2005, **382**, 1567.

10 X. Chen, T. Pradhan, F. Wang, J. S. Kim and J. Yoon, *Chem. Rev.*, 2011, **112**, 1910.

11 (*a*) S. Cai, Y. Lu, S. He, F. Wei, L. Zhao and X. Zeng, *Chem. Commun.*, 2013, **49**, 822; (*b*) L. Duan, Y. Xu and X. Qian, *Chem. Commun.*, 2008, 6339; (*c*) T. Schwarze, W. Mickler, C. Dosche, R. Flehr, T. Klamroth, H.-G. Lohmannsroben, P. Saalfrank and H.-J. Holdt, *Chem.–Eur. J.*, 2010, **16**, 1819; (*d*) M. Santra, S.-K. Ko, I. Shin and K. H. Ahn, *Chem. Commun.*, 2010, **46**, 3964; (*e*) J. R. Matthews, F. Goldoni, H. Kooijman, A. L. Spek, A. P. H. J. Schenning and E. W. Meijer, *Macromol. Rapid Commun.*, 2007, **28**, 1809.

12 (*a*) M. Wang, Y. Yuan, H. Wang and Z. Qin, *Analyst*, 2016, **141**, 832; (*b*) B. Liu, W. Chen, D. Liu, T. Wang, C. Pan, D. Liu, L. Wang and R. Bai, *Sens. Actuators, B*, 2016, **237**, 899; (*c*) W. Liu, J. Jiang, C. Chen, X. Tang, J. Shi, P. Zhang, K. Zhang, Z. Li, W. Dou, L. Yang and W. Liu, *Inorg. Chem.*, 2014, **53**, 12590; (*d*) M. P. Tracey, D. Pham and K. Koide, *Chem. Soc. Rev.*, 2015, **44**, 4769; (*e*) I. S. Turan, O. Yilmaz, B. Karatas and E. U. Akkaya, *RSC Adv.*, 2015, **5**, 34535; (*f*) M. Wang, X. Liu, H. Lu, H. Wang and Z. Qin, *ACS Appl. Mater. Interfaces*, 2015, **7**, 1284; (*g*) M. Arca, C. Caltagirone, G. De Filippo, M. Formica, V. Fusi, L. Giorgi, V. Lippolis, L. Prodi, E. Rampazzo, M. A. Scorciapino, M. Sgarzi and N. Zaccheroni, *Chem. Commun.*, 2014, **50**, 15259.

13 (*a*) H. Cui, H. Chen, Y. Pan and W. Lin, *Sens. Actuators, B*, 2015, **219**, 232; (*b*) H. Li, J. Fan and X. J. Peng, *Chem. Soc.*

Rev., 2013, **42**, 7943; (*c*) B. Qiao, S. Sun, N. Jiang, S. Zhang and X. Peng, *Dalton Trans.*, 2014, 4626; (*d*) H. Li, J. Fan, J. Du, K. Guo, S. Sun and X. Liu, *Chem. Commun.*, 2010, **46**, 1079; (*e*) B. Liu, H. Wang, T. S. Wang, Y. Bao, F. Du, J. Tian, Q. Li and R. Bai, *Chem. Commun.*, 2012, **48**, 2867; (*f*) B. Liu, Y. Bao, F. Du, H. Wang, J. Tian and R. Bai, *Chem. Commun.*, 2011, **47**, 1731.

14 (*a*) E. Pershagen, J. Nordholm and K. E. Borbas, *J. Am. Chem. Soc.*, 2012, **134**, 9832; (*b*) Q. Wu and E. V. Anslyn, *J. Am. Chem. Soc.*, 2004, **126**, 14682; (*c*) W. Chen, B. D. Wright and Y. Pang, *Chem. Commun.*, 2012, **48**, 3824; (*d*) R. Balamurugan, C.-C. Chien, K.-M. Wu, Y.-H. Chiu and J.-H. Liu, *Analyst*, 2013, **138**, 1564; (*e*) H. Chen, W. Lin and L. Yuan, *Org. Biomol. Chem.*, 2013, **11**, 1938; (*f*) L. Zhou, Q. Wang, X.-B. Zhang and W. Tan, *Anal. Chem.*, 2015, **87**, 4503; (*g*) S. Sun, B. Qiao, N. Jiang, J. Wang, S. Zhang and X. Peng, *Org. Lett.*, 2014, **16**, 1132.

15 (*a*) X. Wang, Z. Guo, S. Zhu, H. Tian and W. Zhu, *Chem. Commun.*, 2014, **50**, 13525; (*b*) A. L. Garner, F. Song and K. Koide, *J. Am. Chem. Soc.*, 2009, **131**, 5163; (*c*) F. Song, A. L. Garner and K. Koide, *J. Am. Chem. Soc.*, 2007, **129**, 12354; (*d*) Q. Huang, Y. Zhou, Q. Zhang, E. Wang, Y. Min, H. Qiao, J. Zhang and T. Ma, *Sens. Actuators, B*, 2015, **208**, 22; (*e*) M. S. Baker and S. T. Phillips, *J. Am. Chem. Soc.*, 2011, **133**, 5170; (*f*) J. T. Weiss, J. C. Dawson, K. G. Macleod, W. Rybski, C. Fraser, C. Torres-Sanchez, E. E. Patton, M. Bradley, N. O. Carragher and A. Unciti-Broceta, *Nat. Commun.*, 2014, **5**, 3277.

16 (*a*) A. Rajput and R. Mukherjee, *Coord. Chem. Rev.*, 2013, **257**, 350; (*b*) T. C. Harrop and P. K. Mascharak, *Acc. Chem. Res.*, 2004, **37**, 253; (*c*) P. Kumar and R. Gupta, *Dalton Trans.*, 2016, 18769.

17 (*a*) D. Bansal and R. Gupta, *Dalton Trans.*, 2016, 502; (*b*) D. Bansal, G. Kumar, G. Hundal and R. Gupta, *Dalton Trans.*, 2014, 14865; (*c*) P. Kumar, V. Kumar and R. Gupta, *RSC Adv.*, 2015, **5**, 97874.

18 R. Rusakowicz and A. C. Testa, *J. Phys. Chem.*, 1968, **72**, 2680.

19 P. Pringsheim, *Florescence and Phosphorescence*, Interscience Publishing Co., New York, 1949, p. 333.

20 A. Ganguly, B. K. Paul, S. Ghosh, S. Kar and N. Guchhait, *Analyst*, 2013, **138**, 6532.

21 A. Senthilvelan, I. Ho, K. Chang, G. Lee, Y. Liu and W. Chung, *Chem.–Eur. J.*, 2009, **15**, 6152.

22 H. A. Benesi and J. H. Hildebrand, *J. Am. Chem. Soc.*, 1949, **71**, 2703.

23 (*a*) Y. Furusho, T. Matsuyama, T. Takata, T. Moriuchi and T. Hirao, *Tetrahedron Lett.*, 2004, **45**, 9593; (*b*) Q.-Q. Wang, R. A. Begum, V. W. Day and K. Bowman-James, *Inorg. Chem.*, 2012, **51**, 760.

24 (*a*) J. Zhang, X. Xu, Y. Yuan, C. Yang and X. Yang, *ACS Appl. Mater. Interfaces*, 2011, **3**, 2928; (*b*) Q.-Q. Wang, R. A. Begum, V. W. Day and K. Bowman-James, *J. Am. Chem. Soc.*, 2013, **135**, 17193.

25 R. Zhang, M. Gao, S. Bai and B. Liu, *J. Mater. Chem. B*, 2015, **3**, 1590.

26 T. Mosmann, *J. Immunol. Methods*, 1983, **65**, 55.

27 (*a*) K. Ghosh, S. Kumar, R. Kumar and U. P. Singh, *J. Organomet. Chem.*, 2014, **750**, 169; (*b*) A. N. Dwyer, M. C. Grossel and P. N. Horton, *Supramol. Chem.*, 2004, **16**, 405.

28 C. Liang, W. Bu, C. Li, G. Men, M. Deng, Y. Jiangyao, H. Sun and S. Jiang, *Dalton Trans.*, 2015, 1827.

29 C.-C. Xu, J.-J. Wu, C.-H. Yao, B.-Y. Yu and J.-H. Liu, *Eur. J. Med. Chem.*, 2016, **123**, 763.

30 (*a*) M. Santra, S.-K. Ko, I. Shin and K. H. Ahn, *Chem. Commun.*, 2010, **46**, 3964; (*b*) X. Feng, T. Zhang, J.-T. Liu, J.-Y. Miao and B.-X. Zhao, *Chem. Commun.*, 2016, **52**, 3131.

31 *CrysAlisPro, v. 1.171.33.49b*, Oxford Diffraction Ltd., 2009.

32 G. M. Sheldrick, *Acta Crystallogr., Sect. A: Found. Crystallogr.*, 2008, **64**, 112.

33 O. V. Dolomanov, A. J. Blake, N. R. Champness and M. Schroder, *J. Appl. Crystallogr.*, 2003, **36**, 1283.

34 L. J. Farrugia, *WinGX, v. 1.70*, An Integrated System of Windows Programs for the Solution, Refinement and Analysis of Single- Crystal X-ray Diffraction Data, Department of Chemistry, University of Glasgow, 2003.